APPLIED AND ENVIRONMENTAL MICROBIOLOGY, Nov. 1986, p. 1139–1146
0099-2240/86/111139-08$02.00/0

Vol. 52, No. 5

Structure and Dynamics of Anaerobic Bacterial Aggregates in a Gas-Lift Reactor

H. H. BEEFTINK* AND P. STAUGAARD

Department of Chemical Technology and Biotechnological Centre, University of Amsterdam, 1018 WV Amsterdam, The Netherlands

Received 11 March 1986/Accepted 17 June 1986

Anaerobic mixed-culture aggregates, which converted glucose to acetic, propionic, butyric, and valeric acids, were formed under controlled conditions of substrate feed (carbon limitation) and hydraulic regimen. The continuous-flow system used (anaerobic gas-lift reactor) was designed to retain bacterial aggregates in a well-mixed reactor. Carrier availability (i.e., liquid-suspended sand grains) proved necessary for bacterial aggregate formation from individual cells during reactor start-up. Electron microscopic examination revealed that incipient colonization of sand grains by bacteria from the bulk liquid occurred in surface irregularities, conceivably reflecting local quiescence. Subsequent confluent biofilm formation on sand grains proved to be unstable, however. Substrate depletion in the bulk liquid is assumed to weaken deeper parts of the biofilm due to cellular lysis, after which production of gas bubbles and liquid shearing forces cause sloughing. The resulting fragments, although sand free, were nevertheless large enough to be retained in the reactor and gradually grew larger through bacterial growth and by clumping together with other fragments. In the final steady state, high cell densities were maintained in the form of aggregates, while sand had virtually disappeared due to sampling losses and wash-out. Numerical cell densities within aggregates ranged from 10^{12}/ml at the periphery to very low values in the center. The cells were enmeshed in a polymer matrix containing polysaccharides; nevertheless, carbon sufficiency was not a prerequisite to sustain high hold-up ratios.

Unlike many other bioreactors, wastewater treatment plants are commonly operated on a continuous-flow basis. Such process conditions require retention of microorganisms to obtain elevated biomass concentrations, which improve reactor loading capacity and stability (2, 12, 28). This holds in particular for anaerobic treatment processes, which are characterized by undesirably low biological rate constants.

Retention may be achieved by the adhesion of microorganisms on a stationary support, as in packed-bed reactors. Fluidized-bed bioreactors, on the other hand, rely on the settling of suspended flocs or granules, circumventing the channeling problems frequently encountered with packed-bed configurations.

Clearly, the mechanisms by which bacterial aggregates (flocs, granules, biofilms, etc.) are formed are of particular relevance to the field of wastewater treatment. Electron microscopy may provide important information pertaining to these mechanisms. Reports are available on the microstructure of bacterial aggregates from aerobic or partly aerobic plants (1, 9, 16, 18, 26, 31), but data on completely anaerobic systems are scarce (23). In either case, medium composition and hydraulic regimen are often ill defined and constantly varying, and the reactor contents may be poorly mixed to promote retention.

In the present paper, light and electron microscopic techniques were used to study the structure of mixed-culture aggregates formed under well-defined conditions of substrate feed (carbon limitation) and hydraulic regimen. As a laboratory model process, we investigated the acidification of glucose in a well-defined mineral medium, representing the first stage in the mineralization of carbohydrates in anaerobic digestion. The kinetics, stoichiometry, and physiology of glucose acidification by an anaerobic mixed-culture population obtained from activated sludge as an inoculum are well documented (6, 34; J. C. van den Heuvel, Ph.D. thesis, University of Amsterdam, The Netherlands, 1985).

Aggregates were formed in a novel continuous-flow anaerobic gas-lift reactor (AGLR) with liquid-suspended sand as an adhesion support. The AGLR was designed to enable retention in an otherwise well-mixed reactor, improving mass transport in the liquid phase and allowing high-rate acidification and optimal control of process conditions.

MATERIALS AND METHODS

AGLR. Bacterial aggregates were formed in a continuous-flow AGLR of 1.7 liters working volume (Fig. 1). Before start-up, 20 g of sand (specific mass, 2.65 g/ml; grain size, 250 to 315 μm) was added. Culture gas was recycled continuously to the bottom of the fermentor (4-mm orifice) at a rate of 20 ml/s; a cooling jacket prevented vapor condensation in the recycle line. The reactor was divided in a riser and downcomer section (23-cm^2 cross-sectional area each), and as a result its contents showed a circular flow pattern and were considered well mixed (circulation time, approximately 4 s). To retain sand and bacterial aggregates, liquid was made to leave the reactor in the upward direction through a relatively quiescent effluent section (cross-sectional area, 15 cm^2). A water seal prevented loss of culture gas and entrance of oxygen. Other culture equipment has been described previously (5, 34).

Medium and culture conditions. A simple well-defined inorganic salts medium was used throughout (5, 34). The medium contained glucose at a concentration of 50.5 mmol/liter, allowing carbon- and energy-limited cultivation of microorganisms. Temperature was maintained at 30°C with an incandescent light source (250 W) switched by a contact thermometer; pH was kept at 5.8 by automatic titration with 4 mol of NaOH per liter.

Inoculation and start-up procedure. Prior to inoculation, the reactor was flushed thoroughly with nitrogen gas. As

* Corresponding author.

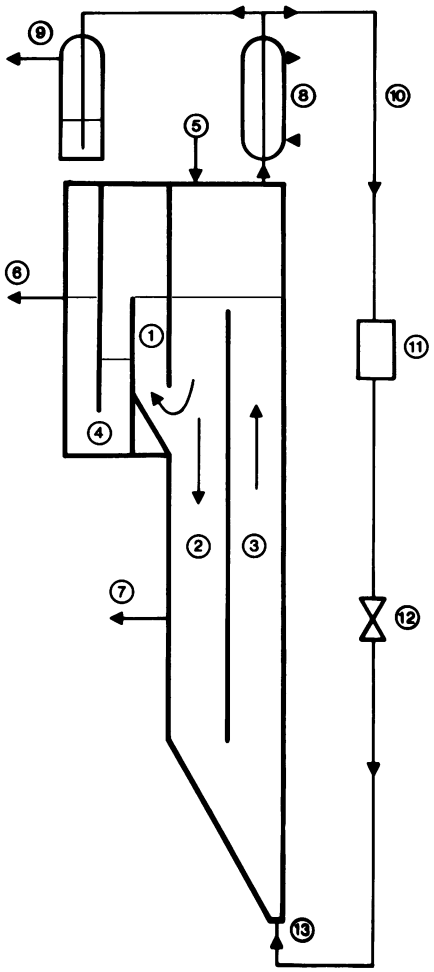

FIG. 1. Schematic view of AGLR configuratrion. 1, effluent section; 2, downcomer; 3, riser; 4, water seal; 5, feed; 6, effluent; 7, sample; 8, cooling jacket; 9, gas outlet; 10, gas recycle; 11, compressor; 12, regulating valve; 13, gas inlet.

inoculum, a fresh sample from an activated-sludge installation treating municipal wastewater was added. When batch operation resulted in complete consumption of glucose, the dilution rate (D) was set at $D = 0.2\ h^{-1}$, i.e., well below the maximum specific growth rate reported for this population in continuous culture ($\mu_{max} = 0.33\ h^{-1}$ [34]). After a steady state was established, the culture still consisting of freely suspended cells, D was raised steeply to $0.6\ h^{-1}$, selecting strongly for the formation of easily retainable aggregates.

TEM. Aggregate-containing samples (20 ml) from the AGLR were decanted, and 20 ml of 0.15-mol/liter NaCl was gently added. Washing with saline was repeated twice and followed by prefixation for 60 min in 2% glutaraldehyde in phosphate buffer (0.1 mol/liter, pH 7.0). Subsequently, the sample was washed three times in a Veronal-acetate buffer (VA) (24) and fixed for 16 h in VA buffer containing 10 g of osmium tetroxide and 3 g of ruthenium red per liter. Dehydration in an ethanol series made up with 1 g of ruthenium red per liter in VA buffer was followed by embedding in araldite CY212. Thin sections were cut with an ultramicrotome, mounted on clean 400-mesh grids or on Formvar-covered 100-mesh grids, and examined in a Philips EM300 transmission electron microscope (TEM) at 40 or 60 kV.

SEM. Samples for scanning electron microscopy (SEM) were washed in saline as described for TEM, dehydrated in an ethanol series made up with 0.15 mol of NaCl per liter, and critical-point dried in liquid carbon dioxide. Dry samples were mounted on SEM stubs with silver paint, sputter-coated with gold-palladium, and examined in a Cambridge Steroscan MkII at 20 or 30 kV or in an ISI DS130 at 3 to 40 kV. Linear dimensions in SEM micrographs were estimated from comparison of the object with marker bars (in micrometers).

Analyses. Fatty acids were determined as described previously (5, 21). Sugars were assayed nonspecifically by the anthrone method, with glucose as the standard (14). Biomass concentrations were determined as dry weight by centrifugation and subsequent lyophilization. Dry-weight pellets were resuspended in 10 g of sodium hypochlorite per liter and incubated for 4 h. Repeated washing with water removed any cellular material from the suspension, and the remaining sand was weighed to correct the initial dry-weight value. The hold-up ratio (retention [R]) of biomass was determined as the ratio of reactor and effluent biomass concentrations.

Alcian blue staining. Smears of aggregates were made on a specimen slide, heat fixed, stained with alcian blue, and examined microscopically (11).

LM. Samples for light microscopy (LM) were fixed and embedded as described for TEM. Semi-thin sections were embedded in Entellan (Merck, Darmstadt, Federal Republic of Germany) on a specimen slide, covered with a cover slip, and examined in a Zeiss Photomicroscope III under dark-field illumination.

Numerical and volumetric cell densities. For cell density measurements, appropriate TEM micrographs (linear magnification, 10^4) were covered with a square lattice (8.65 intersection points per cm^2). The fractional area, A_a, of bacterial cells (i.e., the total area occupied by cells per unit area of the micrograph) was measured as the fraction of intersection points coinciding with bacterial cells. According to the principle of Delesse (29), A_a was used as an unbiased estimate for the fractional volume, V_v (i.e., the total volume of cells per unit volume of aggregate [29]). Calculation of numerical densities (N_v; number of cells per unit volume of aggregate) could not be done straightforwardly due to large variations in cell shape and volume. Therefore, N_v values were estimated as V_v/V_c, V_c being individual cell volumes as estimated from SEM micrographs.

RESULTS

After the shift-up from $D = 0.2\ h^{-1}$ to $D = 0.6\ h^{-1}$, a severe wash-out of the main products from the steady state at $D = 0.2\ h^{-1}$ was observed (i.e., freely suspended bacterial cells, butyrate, and acetate; Table 1). Concomitantly, the concentration of the growth-limiting substrate, glucose, increased sharply. Total wash-out did not occur, however. About 25 mean liquid residence times (τ) after shift-up, the culture started to recover again by forming small but clearly visible aggregates, which were dispersed throughout the reactor liquid; simultaneously, glucose conversion started to increase again. Some 50 τ after shift-up, the start-up procedure was completed and a new steady state had been established, characterized by complete glucose conversion and a considerable hold-up ratio ($R = 6$, reactor biomass concentration was 9 g/liter, effluent biomass concentration

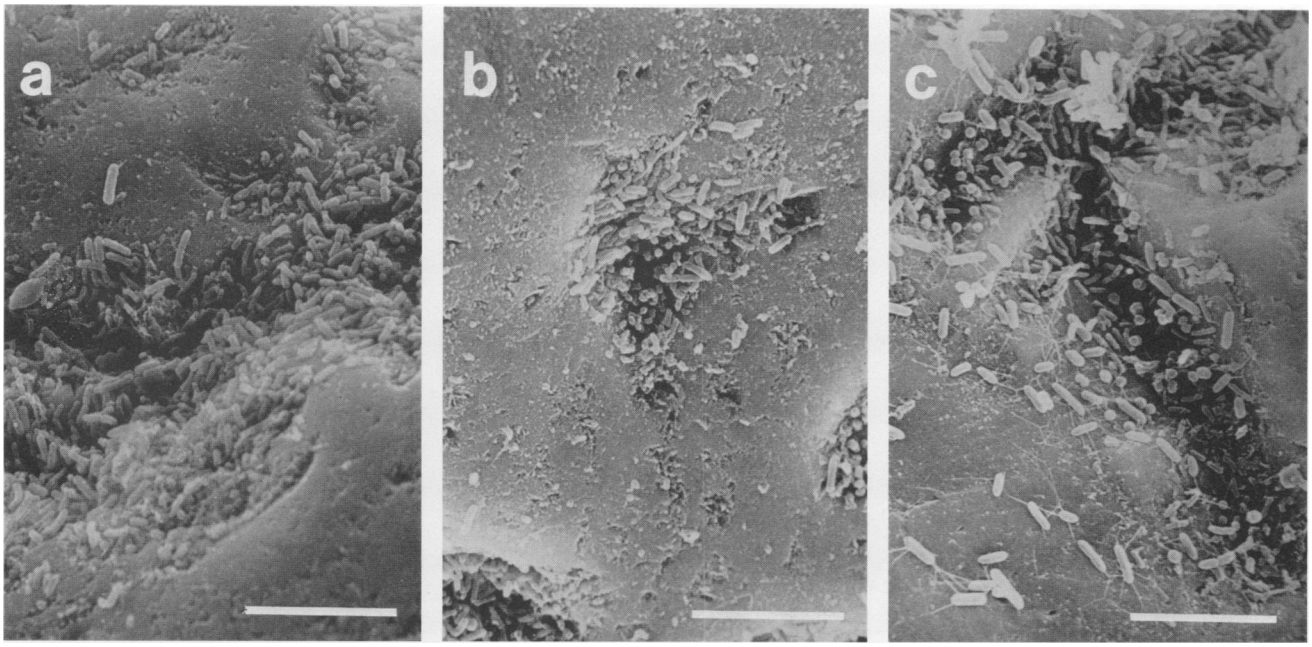

FIG. 2. SEM micrographs of pioneering microcolonies of bacteria on a sand grain at 20 τ after shift-up to $D = 0.6\ h^{-1}$. (a) Mainly rod-shaped bacteria; (b) coccoid and rod-shaped cells; (c) EPS strands connecting bacteria and the sand surface. Bars, 10 μm.

was 1.5 g/liter; also see Table 1). Also, the general metabolic pattern had changed: whereas butyrate and acetate were the main organic acids at $D = 0.2\ h^{-1}$, propionate, valerate, and acetate were predominant at $D = 0.6\ h^{-1}$.

Start-up routines from which sand had been omitted as a control failed to produce aggregates within acceptable time limits. A further indication on the role of sand during start-up was obtained from SEM micrographs. Figures 2 and 3 show very early forms of aggregates, sampled from the reactor 20 τ after the shift-up in dilution rate. The sand is seen to be preferentially colonized in crevices or depressions (Fig. 2). Microcolonies generally were heterogeneous, but sometimes were dominated by a single morphological type. More detailed micrographs indicate that rod-shaped bacteria were linked to each other and to their substratum by a fibrous material (Fig. 3a), whereas coccoid cells showed a different and less abundant type of extracellular material, if any (Fig. 3b). In addition, the sand surface itself was covered with an amorphous, somewhat granular, substance.

Figure 4 shows a further stage of aggregate development (40 τ after shift-up). Often, a confluent biofilm was observed, but occasionally parts had sloughed off the sand surface. In such cases, biofilm thickness was estimated to range from 20 to 50 μm.

Figure 5 shows the general SEM appearance of the final type of aggregate, sampled from the AGLR 80 τ after shift-up, i.e., when the new steady state at $D = 0.6\ h^{-1}$ had become established. Typically, such aggregates had a diameter of 1.0 to 1.5 mm. Although some parts were very smooth, the overall aggregate surface appeared to be divided into subregions, which were separated by fissions and irregularities.

TABLE 1. Comparison of fermentation products in steady states with freely suspended bacterial cells ($D = 0.2\ h^{-1}$) and with bacterial aggregates ($D = 0.6\ h^{-1}$)[a]

D (h^{-1})	Product (mmol/liter)				R
	Acetate	Propionate	Butyrate	Valerate	
0.2	18	4	23	0	1
0.6	17	29	9	9	6

[a] D, Dilution rate; R, hold-up ratio.

TEM sections were also prepared from steady-state aggregates. Unexpectedly, no difficulties were encountered in sectioning, obviously indicating the absence of sand grains in the center of these aggregates. Such ruthenium-stained TEM sections are shown in Fig. 6. At high magnification (Fig. 6a), a considerable amount of extracellular ruthenium-positive polymeric substance (EPS) was seen, which was intimately connected with gram-negative rod-shaped bacteria. However, other morphologically distinct, rod-shaped cells were often seen to lack directly adhering EPS and to lie in a clear zone (Fig. 6b). The same held for gram-positive coccoid cells, which at lower magnification were observed to form microcolonies within areas dominated by EPS-forming rod-shaped cells (Fig. 6c).

Apart from its reaction to ruthenium, a further indication of the chemical nature of the EPS was obtained from anthrone determinations. Steady-state aggregates contained 15 to 25% (wt/wt) sugar (expressed as glucose on a dry-weight basis), whereas this figure was three times lower for freely suspended cells taken from the AGLR at a low dilution rate ($D = 0.2\ h^{-1}$). In addition, stained smears of steady-state aggregates clearly indicated the presence of alcian blue-positive extracellular material (not shown).

From low-magnification TEM micrographs (e.g., Fig. 6c), the fractional bacterial volume within aggregates (V_v) was calculated to range from 0.21 to 0.27 for steady-state aggregates. Based on individual cell volumes (V_c) of 0.2 to 0.5 μm^3, the numerical cell densities, N_v, were estimated as 0.4×10^{12} to $1.4 \times 10^{12}\ ml^{-1}$.

As with TEM, sand grains were not encountered in sectioning for LM. A general LM overview of a steady-state aggregate is shown in Fig. 7a. Towards the center, a deteriorated appearance with very low cell densities was ob-

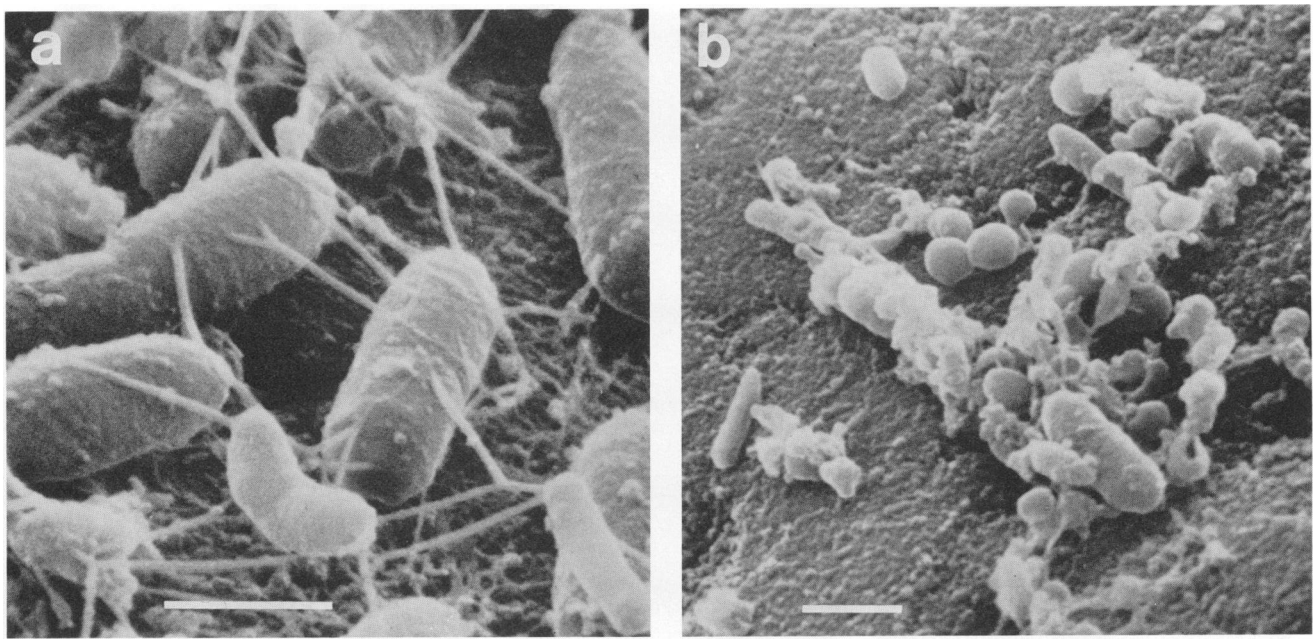

FIG. 3. SEM details of pioneering cells on sand grain at 20 τ after shift-up. (a) Strandlike EPS between rod-shaped cells and sand surface; (b) coccoid cells, possessing less extensive EPS. Bars, 1 μm.

served. Furthermore, aggregates consisted of several subaggregates. At the aggregate-liquid interface (Fig. 7b) and at separations between subaggregates (Fig. 7c), population differences could be observed microscopically. Often, microcolonies appeared to penetrate from the surface into deeper regions (Fig. 7c).

DISCUSSION

During start-up, sand grains were essential for aggregate formation, since omission of sand frustrated the start-up procedure. Due to its dimensions and specific weight, sand has a relatively long residence time in the AGLR, providing an excellent substratum for bacterial attachment and subsequent biofilm formation. As apparent from the absence of hold-up in the steady state at a low dilution rate ($D = 0.2\ h^{-1}$, $R = 1$) and from the initial wash-out of biomass after the shift-up in $D = 0.6\ h^{-1}$, individual bacterial cells are not retained by the settling device. Depending on the fluid behavior in the effluent section (e.g., turbulence), retention of particulate material is not only determined by the settling velocity, but has stochastic characteristics as well. However, if settling velocities (v^{∞}) are high with respect to the mean upward liquid velocity in the effluent section, retention becomes increasingly efficient. The liquid velocity may be calculated to average 0.2 mm/s at $D = 0.6\ h^{-1}$, i.e., largely exceeding v^{∞} for individual bacterial cells. With sand as the adhesion support, however, v^{∞} values exceeding 0.2 mm/s

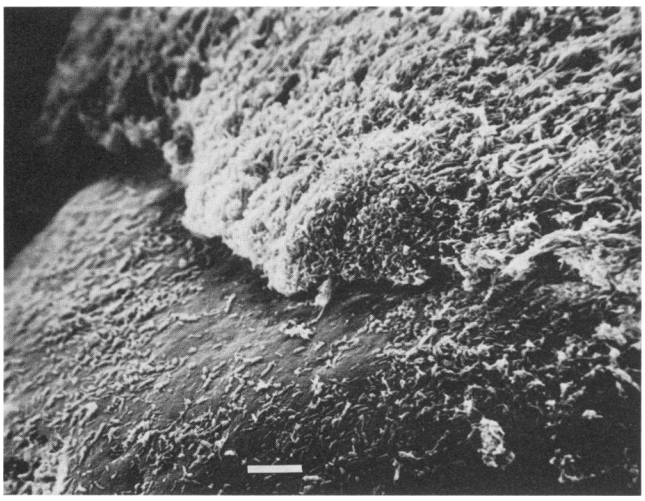

FIG. 4. SEM view of biofilm-covered sand grain at 30 τ after shift-up. Part of the sand is exposed as result of biofilm sloughing. Bar, 10 μm.

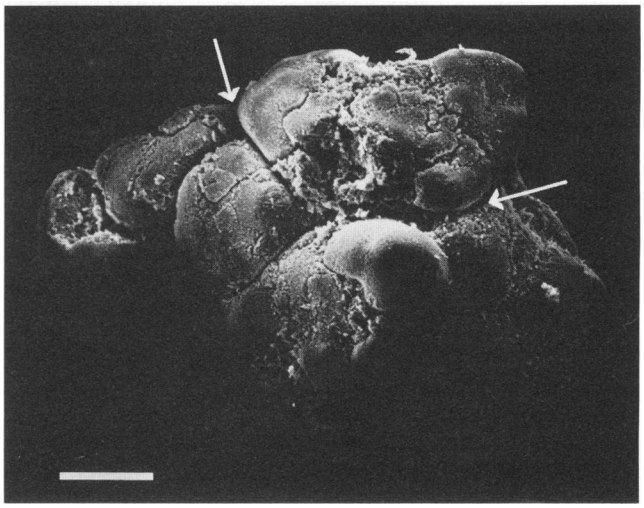

FIG. 5. Overall SEM appearance of steady-state aggregate at 80 τ after shift-up. Fissures and irregularities (arrows) between subaggregates, which are rather smooth. Bar, 500 μm.

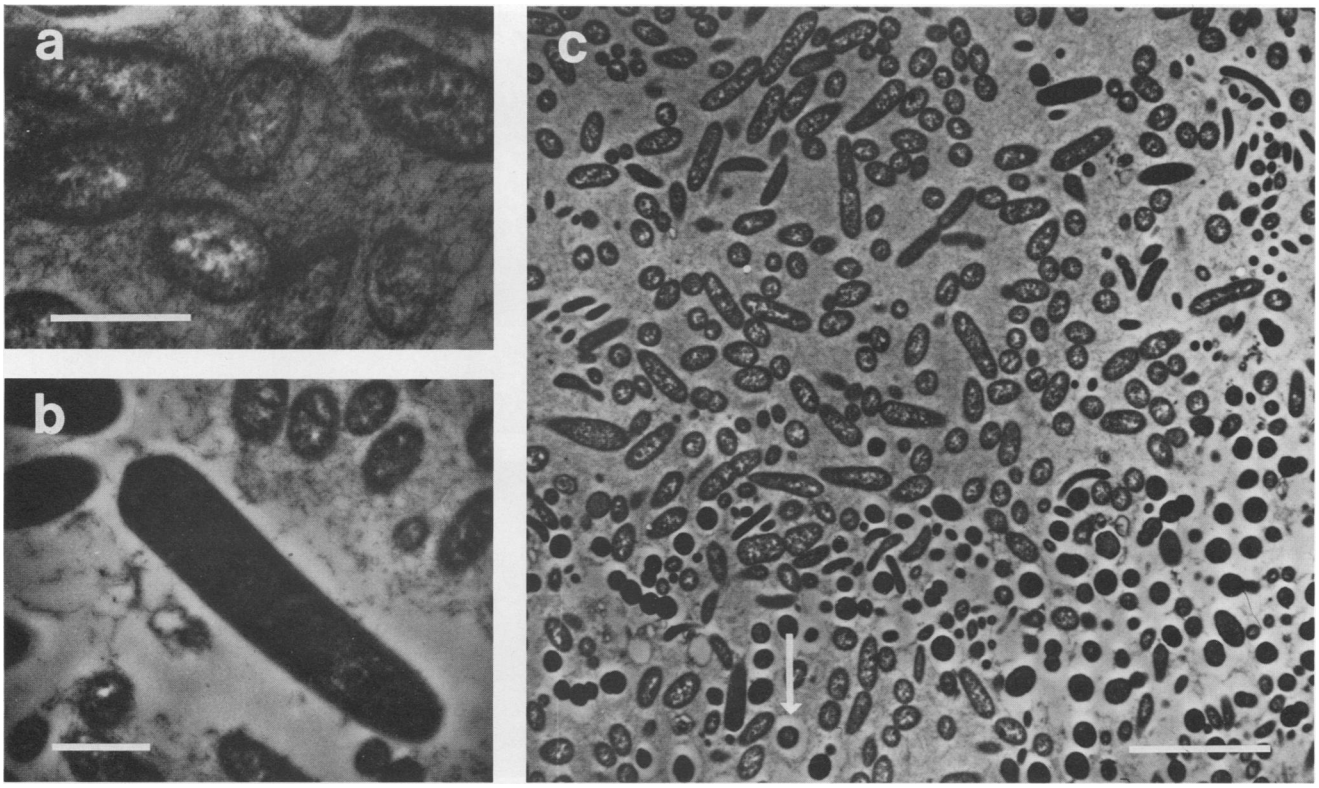

FIG. 6. Ruthenium red-stained TEM section through a steady-state aggregate at 80 τ after shift-up. (a) Gram-negative rod-shaped bacteria are seen to be intimately connected to EPS (bar, 1 μm); (b) bacterium in a clear zone without EPS (bar, 1 μm); (c) same aggregate at low magnification. Coccoid cells are seen to be surrounded by a clear zone (arrow) and may occupy larger areas (lower right) (bar, 5 μm).

are easily attainable for sand-biomass aggregates: v^{∞} values for bare sand grains may be calculated to average 30 mm/s.

With the aid of SEM techniques, the onset of biofilm formation was observed as microcolonies, preferentially located in depressions or crevices in the surface of sand grains. A similar phenomenon has been observed with marine sediments and was ascribed to mechanical damaging by adjacent sand grains (30). In the present case, however, surface irregularities of sand grains probably create regions of low liquid turbulence and thus of low shearing forces. Such forces are reported to remove attached bacteria from inert surfaces (22, 27).

Notwithstanding these shearing forces, a confluent biofilm developed from these microcolonies 40 τ after start-up. For several reasons, however, it is concluded that such biofilm-covered sand grains only represent an intermediate type of aggregate and that eventual steady-state aggregates are essentially free of sand and are of a quite dynamic nature. First of all, sand grains were not detected in sectioned steady-state aggregates at 80 τ for TEM and LM. Furthermore, SEM micrographs of the intermediate type of aggregates at 40 τ showed severe sloughing of biofilm, exposing the sand surface. It is postulated therefore that the settling velocity of the biofilm fragments detached by sloughing is high enough to allow efficient retention even though they do not contain any sand. Such fragments would gain again in size by bacterial growth. Notwithstanding its high v^{∞} value, sand gradually disappears from the reactor, since it, unlike biomass, is not regenerated in situ. Effluent samples did contain small amounts of sand, but the major losses of sand are attributed to sampling of the reactor contents. From the biomass determination used, the remaining sand in the reactor at 60 τ after shift-up was estimated to be less than 10% of the initial amount. In summary, detachment of rather large biofilm fragments from sand grains on the one hand and sampling losses and wash-out of sand on the other result in a transition from sand-containing aggregates to aggregates without sand.

A further complication has to be taken into account. If aggregate-containing samples from the reactor were left to stand for 15 min, aggregates were found to stick together. Therefore, in situ clumping of small aggregates into larger units is conceivable. In this respect, it is of interest that LM and SEM micrographs of steady-state aggregates revealed that they consisted of several smaller subunits.

LM micrographs (Fig. 7) showed cell densities to be high at the periphery and low in the center of aggregates. Conceivably, these low densities reflect a locally insufficient glucose supply caused by diffusional limitation. As a result, maintenance requirements are not met and cell lysis occurs. Consequently, the mechanical strength of aggregates is affected, and the combination of this internal weakening by substrate deficiency and external shearing forces arising from liquid turbulence may result in fragmentation. In addition, fragmentation may be aggravated by the production of gaseous metabolites within the aggregates. Such mechanical effects by gas bubbles arising within biofilms have been postulated before (3, 13, 15, 17, 20). An identical mechanism is thought to underlie the above-mentioned detachment of biofilm fragments from sand grains.

The importance of cell lysis can also be inferred from the abundant production of valeric acid coinciding with aggre-

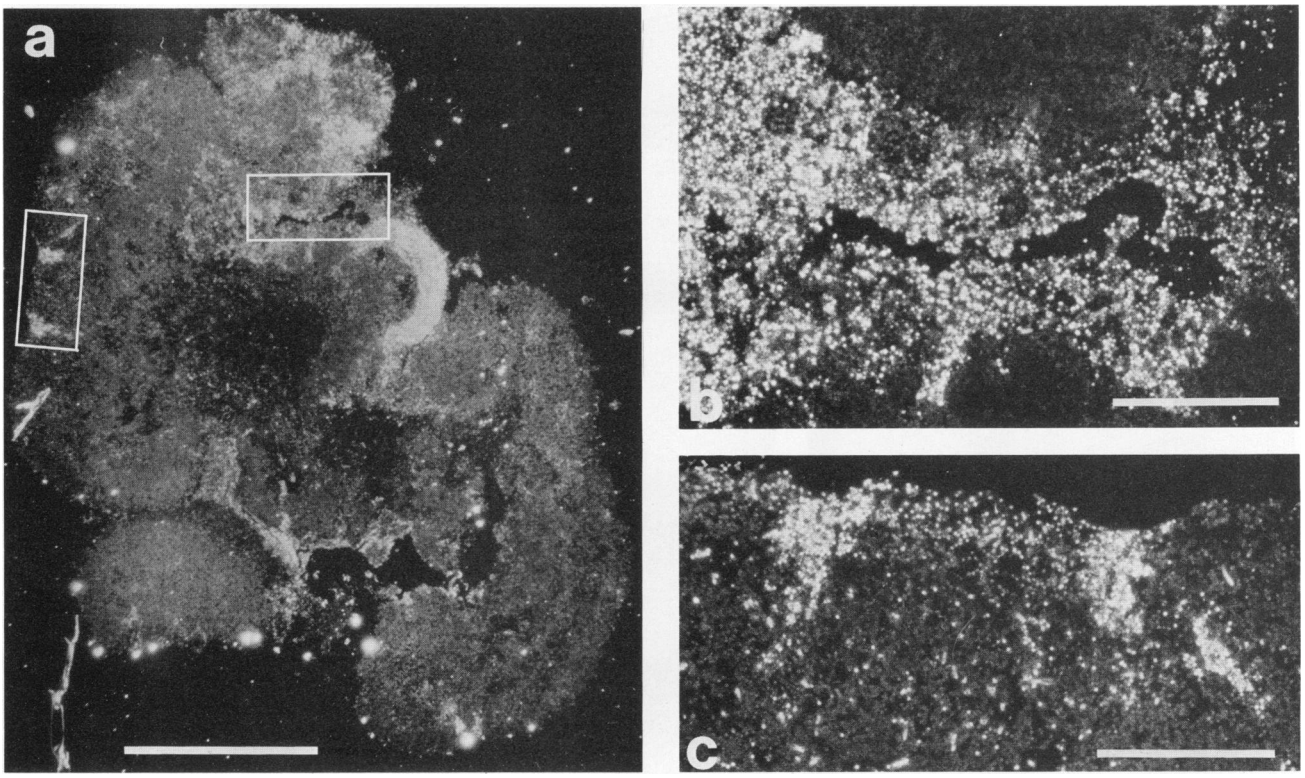

FIG. 7. (a) Low-magnification LM view under dark-field illumination of a complete steady-state aggregate (80 τ after shift-up). An area of low bacterial density in the center and various subaggregates can be observed. Bar, 250 μm. (b) High-magnification detail of right-hand boxed area in panel a. The fissure between two subaggregates is seen to be occupied by a microscopically distinct population. Bar, 50 μm. (c) High-magnification LM micrograph of the outer boundary of an aggregate (left-hand boxed area in panel a). The peripheral region is seen to be occupied by a distinct microbial population. Bar, 50 μm.

gate formation. With glucose as a substrate, valeric acid generally is not a major fermentation product. Large amounts of valeric acid, on the other hand, are often found in the fermentation of complex macromolecules. The latter type of substrate would be amply available as a result of cell lysis.

Data on cellular densities, which are relevant to future model calculations on aggregate performance, were obtained from TEM micrographs. Morphometric measurements revealed V_v values ranging from 0.21 to 0.27, whereas N_v values between 0.4×10^{12} and 1.4×10^{12} ml^{-1} were measured. These V_v and N_v estimates are probably not mean values for the whole aggregate, since selection of TEM micrographs tends to be biased against the center of aggregates, with its low cellular densities. Furthermore, inaccuracy may arise from shrinking of samples in the dehydration procedure. However, the present data are in good agreement with the data of Strand et al. (25), who reported viable counts of 10^{11} to 10^{12} ml^{-1} for partly aerobic biofilms. A large discrepancy, on the other hand, exists with the data of Trulear and Characklis (27; c.f. reference 4), who reported viable counts as low as 10^4 ml^{-1}. Surprisingly, the latter value is several orders of magnitude lower than the common density of freely suspended bacteria in liquid culture.

TEM and SEM micrographs indicated that most cells were intimately enmeshed in an extensive matrix of EPS. However, not all population members were equally active in EPS formation, since some rod-shaped and coccoid cells in particular were seen to be lying in an EPS-free zone. Such nonadhering cells may have been entrapped from the bulk liquid during biofilm formation, a phenomenon which has been reported before (7). Since formation of aggregates in the AGLR implies selection for adhesive properties, the observed metabolic shift from butyrate to propionate production after aggregate formation could at least partly be due to a shift in population composition. Entrapment of nonadhering, butyrate-producing bacteria in films of propionate-forcing organisms could explain the continuing production of moderate amounts of butyrate. At present, however, no evidence is available that biofilm-entrapped cells indeed produce butyric acid.

The appearance of EPS in electron microscopic preparations was strongly dependent on the procedure used. Whereas TEM micrographs showed very thin and almost amorphous fibrils, the EPS in SEM micrographs was seen as thick strands. These differences are generally believed to reflect different extents of dehydration artifacts of the EPS, which is quite diffuse in vivo.

The positive reaction of EPS to ruthenium red as well as to alcian blue and the rather high sugar content of whole aggregates from anthrone analysis all indicate that sugars are an important component of EPS. This is in agreement with previously published findings on various bacterial aggregates (8, 10). In view of the high sugar content of EPS, various authors have postulated carbon sufficiency to be a prerequisite for extensive EPS formation and bacterial adhesion (19,

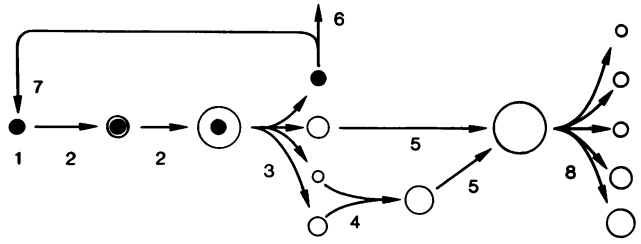

FIG. 8. Working hypothesis of the development of anaerobic mixed-culture aggregates: 1, bare sand grain; 2, progressive biofilm formation on sand grain; 3, detachment of biofilm into smaller fragments; 4, clumping of small fragments; 5, growth of aggregates; 6, loss of sand; 7, recolonization of sand; 8, fragmentation of large aggregates.

32, 33). In the present case, however, considerable hold-up ratios could be sustained in the final steady state regardless of glucose limitation.

In summary, the working hypothesis outlined above implies that final steady-state aggregates are of a very dynamic nature. They do not reach a true steady-state condition, but gain in size continuously by bacterial growth and a tendency to stick to each other. On the other hand, their maximum diameter is limited by disintegration of large aggregates. As an important consequence, the relative position of an individual bacterium within an aggregate is continuously changing, and so are its environmental conditions. Figure 8 shows a schematic representation of these processes. A continuous distribution of aggregate diameters over a wide range is thus predicted. Quantitative data on diameter distributions will be published separately.

The dynamic behavior of bacterial aggregates as described here quite likely is applicable to other reactor configurations in which biomass is retained. However, the relative contributions of individual processes (shearing forces, cell lysis, gas production, etc.) may depend on the specific experimental conditions used (reactor, substrate, bacterial species, etc.).

ACKNOWLEDGMENTS

The expert technical assistance in electron microscopy of C. Bakker (University of Amsterdam) and in light microscopy of P. Room (Free University, Amsterdam) is gratefully acknowledged.

LITERATURE CITED

1. **Alleman, J. E., J. A. Veil, and J. T. Canaday.** 1982. Scanning electron microscope evaluation of rotating biological contactor biofilm. Water Res. **16**:543–550.
2. **Atkinson, B.** 1981. Immobilized biomass—a basis for process development in wastewater treatment, p. 22–34. *In* P. F. Cooper and B. Atkinson (ed.), Biological fluidised bed treatment of water and wastewater. Ellis Horwood, Chichester, U.K.
3. **Atkinson, B., G. M. Black, P. J. S. Lewis, and A. Pinches.** 1979. Biological particles of given size, shape, and density for use in biological reactors. Biotechnol. Bioeng. **21**:193–200.
4. **Characklis, W. G., and K. E. Cooksey.** 1983. Biofilms and microbial fouling. Adv. Appl. Microbiol. **29**:93–138.
5. **Cohen, A., A. M. Breure, J. G. van Andel, and A. van Deursen.** 1980. Influence of phase separation on the anaerobic digestion of glucose. I. Maximum *COD*-turnover rate during continuous operation. Water Res. **14**:1439–1448.
6. **Cohen, A., J. M. van Gemert, R. J. Zoetemeyer, and A. M. Breure.** 1984. Main characteristics and stoichiometric aspects of acidogenesis of soluble carbohydrate containing wastewaters. Proc. Biochem. **19**:228–232.
7. **Costerton, J. W., G. G. Geesey, and K.-J. Cheng.** 1978. How bacteria stick. Sci. Am. **238**:86–95.
8. **Deinema, M. H., and L. P. T. M. Zevenhuizen.** 1971. Formation of cellulose fibrils by gram-negative bacteria and their role in bacterial flocculation. Arch. Mikrobiol. **78**:42–57.
9. **Eighmy, T. T., D. Maratea, and P. L. Bishop.** 1983. Electron microscopic examination of wastewater biofilm formation and structural components. Appl. Environ. Microbiol. **45**:1921–1931.
10. **Fletcher, M., and G. D. Floodgate.** 1973. An electron-microscopic demonstration of an acidic polysaccharide involved in the adhesion of a marine bacterium to solid surfaces. J. Gen. Microbiol. **74**:325–334.
11. **Gurr, E.** 1965. Alcian blue for bacterial polysaccharides and capsules, p. 170–171. *In* E. Gurr (ed.), The rational use of dyes in biology. Leonard Hill, London.
12. **Hamer, G.** 1982. Recycle in fermentation processes. Biotechnol. Bioeng. **24**:511–531.
13. **Harremoës, P., J. la Cour Jansen, and G. Holm Kristensen.** 1980. Practical problems related to nitrogen buble formation in fixed film reactors. Prog. Water Technol. **12**:253–269.
14. **Jermyn, M. A.** 1975. Increasing the sensitivity of the anthrone method for carbohydrate. Anal. Biochem. **68**:332–335.
15. **Kierstan, M., and C. Bucke.** 1977. The immobilization of microbial cells, subcellular organelles, and enzymes in calcium alginate gels. Biotechnol. Bioeng. **19**:387–397.
16. **Kinner, N. E., D. L. Balkwill, and P. L. Bishop.** 1983. Light and electron microscopic studies of microorganisms growing in rotating biological contactor biofilms. Appl. Environ. Microbiol. **45**:1659–1669.
17. **Krouwel, P. G., and N. W. F. Kossen.** 1980. Gas production by immobilized microorganisms: theoretical approach. Biotechnol. Bioeng. **22**:681–687.
18. **Mack, W. N., J. P. Mack, and A. O. Ackerson.** 1975. Microbial film development in a trickling filter. Microb. Ecol. **2**:215–226.
19. **Matson, J. V., and W. G. Characklis.** 1976. Diffusion into microbial aggregates. Water Res. **10**:877–885.
20. **Nilsson, I., S. Ohlson, L. Häggström, N. Molin, and K. Mosbach.** 1980. Denitrification of water using immobilized *Pseudomonas denitrificans* cells. Eur. J. Appl. Microbiol. Biotechnol. **10**:261–274.
21. **Ottenstein, D. M., and D. A. Bartley.** 1971. Separation of free acids C_2-C_5 in dilute aqueous solution column technology. J. Chromatogr. Sci. **9**:673–681.
22. **Powell, M. S., and N. K. H. Slater.** 1982. Removal rates of bacterial cells from glass surfaces by fluid shear. Biotechnol. Bioeng. **24**:2527–2537.
23. **Robinson, R. W., D. E. Akin, R. A. Nordstedt, M. V. Thomas, and H. C. Aldrich.** 1984. Light and electron microscopic examinations of methane-producing biofilms from anaerobic fixed-bed reactors. Appl. Environ. Microbiol. **48**:127–136.
24. **Ryter, A., E. Kellenberger, A. Birch-Andersen, and O. Maaløe.** 1958. Etude au microscope électronique de plasmas contenant de l'acide désoxyribonucléique. I. Les nucléoides des bactéries en croissance active. Z. Naturforschung **13B**:597–605.
25. **Strand, S. E., A. J. McDonnell, and R. F. Unz.** 1985. Concurrent denitrification and oxygen uptake in microbial films. Water Res. **19**:335–344.
26. **Tago, Y., and K. Aida.** 1977. Exocellular mucopolysaccharide closely related to bacterial floc formation. Appl. Environ. Microbiol. **34**:308–314.
27. **Trulear, M. G., and W. G. Characklis.** 1982. Dynamics of biofilm processes. J. Water Pollut. Control Fed. **54**:1288–1301.
28. **Van den Heuvel, J. C., and R. J. Zoetemeyer.** 1982. Stability of the methane reactor: a simple model including substrate inhibition and cell recycle. Proc. Biochem. **17**:14–19.
29. **Weibel, E. R.** 1979. Stereological methods, vol. 1: practical methods for biological morphometry. Academmic Press, Ltd., London.
30. **Weise, W., and G. Rheinheimer.** 1978. Scanning electron microscopy and epifluorescence investigation of bacterial colonization of marine sand sediments. Microb. Ecol. **4**:175–188.
31. **Wheatley, A. D.** 1981. Investigations into the ecology of biofilms

in waste treatment using scanning electron microscopy. Environ. Technol. Lett. **2**:419–424.

32. **Williams, A. G., and J. W. T. Wimpenny.** 1978. Exopolysaccharide production by *Pseudomonas* NCIB11264 grown in continuous culture. J. Gen. Microbiol. **104**:47–57.
33. **Zevenhuizen, L. P. T. M.** 1981. Cellular glycogen, β-1,2,-glucan, poly-β-hydroxybutyrate and extracellular polysaccharides in fast growing species of *Rhizobium*. Antonie van Leeuwenhoek J. Serol. Microbiol. **47**:481–497.
34. **Zoetemeyer, R. J., J. C. van den Heuvel, and A. Cohen.** 1982. pH influence on acidogenic dissimilation of glucose in an anaerobic digestor. Water Res. **16**:303–311.